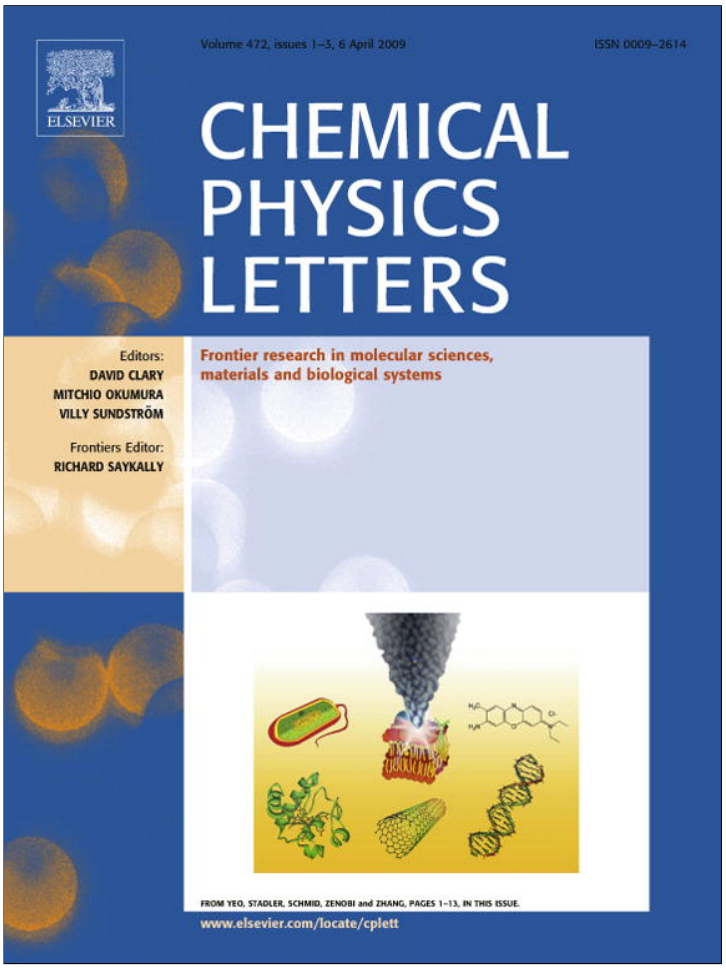

Chemical Physics Letters 472 (2009) 48–54

Contents lists available at ScienceDirect

Chemical Physics Letters

journal homepage: www.elsevier.com/locate/cplett

Investigation of probe molecule–polymer interactions

E. Braeken [a], P. Marsal [b], A. Vandendriessche [a], M. Smet [a], W. Dehaen [a], R.A.L. Vallée [c,*], D. Beljonne [b], M. Van der Auweraer [a]

[a] Department of Chemistry and Institute of Nanoscale Physics and Chemistry, Katholieke Universiteit Leuven, Celestijnenlaan 200F, B-3001 Heverlee, Belgium
[b] Laboratory for Chemistry of Novel Materials, University of Mons-Hainaut, Place du Parc 20, B-7000 Mons, Belgium
[c] Centre de Recherche Paul Pascal (CNRS), 115 Avenue du docteur Albert Schweitzer, F-33600 Pessac, France

ARTICLE INFO

Article history:
Received 8 January 2009
In final form 27 February 2009
Available online 5 March 2009

ABSTRACT

We probe the single molecule–polymer interactions for two types of carbocyanine dyes having the same conjugated core but different side chains. Several conformers of the conjugated core were observed and could be assigned owing to quantum chemistry and molecular dynamics simulations. The relative population of the various conformers is different for the two types of probe molecules in (non) annealed films. The presented results and discussion, of high interest from a fundamental point of view, might also be of primordial importance for the understanding of the plasticizing effect in polymers on a very local scale.

1. Introduction

Most single molecule fluorescence spectroscopy experiments have been performed with the probe molecules embedded in polymer films in order to immobilize them and investigate opto-electronic properties, like the efficiency of resonance energy transfer or electron transfer between different chromophoric parts of the overall system [1–3]. Nowadays, the fluorophores are more and more used to investigate the polymer properties, especially around the glass transition temperature. In order to measure the rotational dynamics of molecules and the related polymer mobility, polarization measurements [4–6] have been performed. Schob et al. [4] and Deschenes et al. [5] found evidence for static and dynamic heterogeneity in the supercooled regime. Zondervan et al. [6] investigated the rotational motion of perylene diimide in glycerol. The results of their experiments lead them to assume that glycerol consists of heterogeneous liquid pockets separated by a network of solid walls, an assumption that was further confirmed by conducting rheology measurements of glycerol at very weak stresses [7]. These polarization techniques typically allow for the detection of a two-dimensional projection of the real three-dimensional motion. The latter can be measured by using either an annular illumination technique [8], a defocused wide-field imaging technique [9–11] or by directly recording the emission pattern in the objective's back focal plane [12] or in the presence of aberrations [13]. Besides these techniques based on orientational dynamics, the fluorescence lifetime of a single dye molecule has been shown to be able to probe the dynamics of the probe surrounding polymer environment either in the glassy state [14–18] or in the supercooled regime [15,19]. Finally, the fluorescence lifetime observable has been used to probe the interaction of small probe molecules with polymer chains. Indeed, we recently investigated the interaction between the carbocyanine dye 1,1′-dioctadecyl-3,3,3′,3′-tetramethylindodicarbocyanine (DiD) and poly(styrene) (PS) polymer chains [18]. The main results of this investigation were the following: the measured fluorescence lifetimes and spectral widths of the DiD molecules were clearly dispersed in bimodal distributions. Quantum chemical calculations showed that the bimodal character could be attributed to two classes of conformations i.e. planar and non planar conformers. Two different planar conformers and only one type of non planar conformers were experimentally observed and clearly assigned owing to these quantum chemical calculations. The main difference between the two planar conformations was in the position of the alkyl chains with respect to the conjugated core: the alkyl chains lay on either the same side of the conjugated backbone (syn-conformer) or the opposite side (anti-conformer), the latter being true as well in the case of the non planar conformer. We compared the experimentally observed fluorescence lifetimes, widths of their distributions, obtained by recording them successively in time, and emission spectra of the probe molecules to dedicated molecular dynamics simulations. This allowed us to make statements about the local interaction of the probe and its local surrounding. For instance, in the case of the syn-conformer, steric hinder between the two alkyl chains (intramolecular interaction) lead to a decreased packing density and an increased local free volume while the alkyl chains of the anti-conformer could interact more strongly with the surrounding PS chains (inter solute–solvent interaction), thereby lowering the local free volume. This type of investigation is not only of interest for its fundamental nature, but is also useful in order to investigate

* Corresponding author.
E-mail addresses: vallee@crpp-bordeaux.cnrs.fr (R.A.L. Vallée), mark.vanderauweraer@chem.kuleuven.be (M. Van der Auweraer).

0009-2614/$ - see front matter © 2009 Elsevier B.V. All rights reserved.
doi:10.1016/j.cplett.2009.02.083

very locally the effect of the introduction of additives in a polymer matrix (plasticizing effect) on the polymer mobility and the corresponding variation of the glass transition temperature. In this Letter, in order to further investigate this kind of probe molecule – surrounding polymer matrix interaction, we make use of two different probe molecules which, while having the same conjugated core, present different side chains able to interact specifically with the surrounding poly(styrene) chains. Both molecules are carbocyanine dyes with a shorter conjugated backbone than the previously investigated DiD molecule. Due to this shortened backbone, the side chains substituted on the nitrogen atoms (Fig. 1a) are closer, which makes it easier for them to interact. Both molecules differ in the nature of the side chains grafted on the nitrogen atoms. One dye has alkyl chains (1,1′-didodecyl-3,3,3′,3′-tetramethylindo-carbocyanine perchlorate, DiIC12) while the other one has oligostyrene chains (DiIsty) substituted on the nitrogen atoms. These molecules are expected to interact differently with the surrounding PS chains, owing to the differences in rigidity, steric hinder and solvation of the side chains. The schematic structure of the dye molecules is visualized in Fig. 1a. Both types of probe molecules were investigated by fluorescence spectroscopy at the bulk and single molecule level. On the single molecule level, both non annealed and annealed samples were measured. In the non annealed case, the memory of the solvent is retained, which gives rise to results significantly different to those obtained if a chance is given to the chains to relax, i.e. after annealing. For both dyes, i.e. DiIC12 and DiIsty, bimodal distributions of fluorescence lifetimes are obtained both for the non annealed and the annealed samples. In the latter case, the distributions for both dyes are very similar, while they exhibit different characteristics in the non annealed case. Based on quantum chemical calculations, these distributions could be assigned to different conformers of DiIC12 and DiIsty.

2. Materials and methods

2.1. Experimental section

Steady state absorption and emission spectra of DiIsty and DiIC12 in toluene were recorded for concentrations of ca. 10^{-6} M. The absorption measurements were carried out on a Perkin Elmer Lambda 40 UV/Vis spectrophotometer. Corrected emission spectra were recorded on a SPEX fluorolog. For the single molecule measurements, a PS ($M_w = 250000$) solution of 10 mg/ml in toluene was used to make solutions of nanomolar (10^{-9} M) concentrations of DiIC12 and DiIsty in PS. The samples were prepared by spincoating the solutions at a rate of 1000 rpm on glass substrates. The non annealed samples were measured immediately after spincoating. To anneal the samples, they were put in the oven at a temperature of 373 K (T_g of the PS used). After five minutes the oven was switched off and let closed in order to allow for a slow decrease of its temperature to room temperature. The single molecule measurements were performed with a confocal microscope setup. The excitation wavelength was set to 543 nm and the laser power was set to 1 μW at the entrance of the microscope. The excitation at 543 nm (8 MHz, 1.2 ps FWHM) was obtained from the frequency-doubled output of an optical parametric oscillator (GWU)

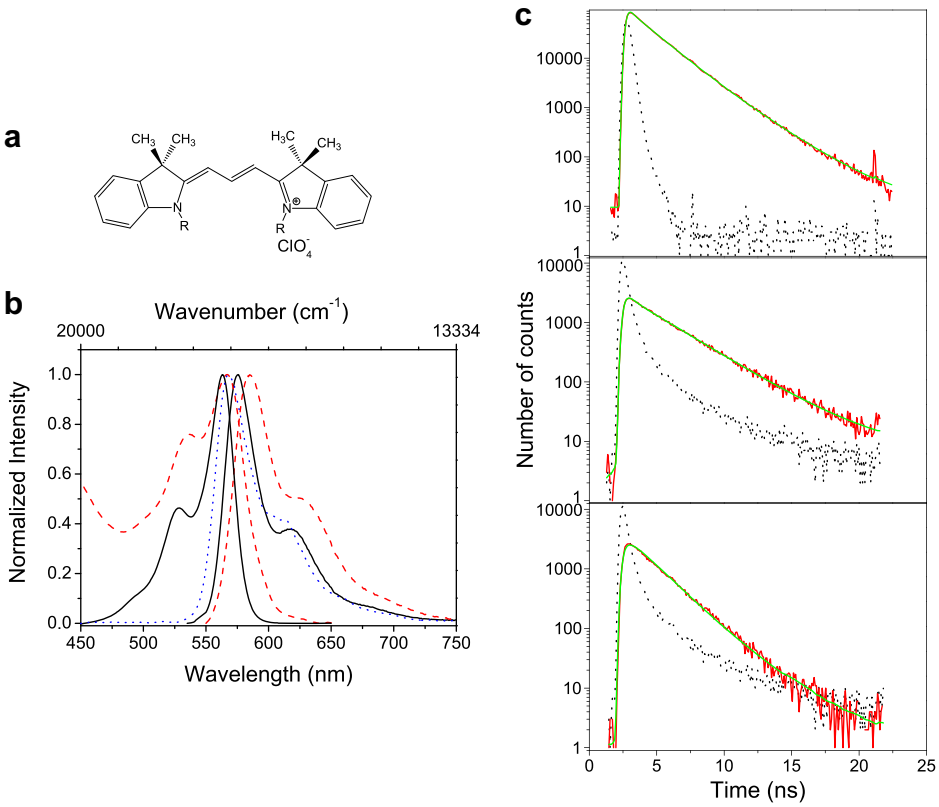

Fig. 1. (a) Schematic structure of the indocarbocyanine dye molecules with R = $C_{12}H_{25}$ for DiIC12 and R = $[CH_2CHC_6H_5]_{23}$ for DiIsty. (b) Normalized absorption and emission spectra of DiIC12 (black solid line) and DiIsty (red dashed line) in toluene. For the sake of comparison, the blue dotted line corresponds to the emission spectrum of a film obtained by spincoating a bulk solution of DiIC12 in PS/toluene onto a glass substrate and further annealed. (c) Fluorescence decay profiles for a diffraction limited volume of a film spincoated from the bulk solution of DiIC12 in PS/toluene (top, this decay profile exhibits two fluorescence decay times: $\tau = 1.8$ ns and $\tau = 2.8$ ns), a single molecule with a long fluorescence lifetime (middle, single exponential decay with $\tau = 2.8$ ns) and a single molecule with a short fluorescence lifetime (bottom, single exponential decay with $\tau = 1.8$ ns). The dotted lines are the instrumental response functions. (For interpretation of the references to color in this figure legend, the reader is referred to the web version of this article.)

pumped by a Ti:sapphire laser (Tsunami, Spectra Physics). The emission light was equally split into two parts. The fluorescence lifetime was measured with an avalanche photodiode (SPCM-AQ-15, EG & G Electro Optics) equipped with a time correlated single photon counting card (TCSPC card, Becker & Hickl GmbH, SPC 630) used in FIFO mode. The bin times that were used to build the decay profiles for the molecules were set to 100 ms in order to have at least 500 counts in the decay. This is the minimum number of counts that is needed to fit the decays using the maximum likelihood estimation method [20]. The emission spectra were recorded with a charge coupled device (CCD) camera with an integration time of 3 s. For DiIC12, the emission spectra and fluorescence decay times of a bulk sample, obtained by spin-coating a solution of DiIC12 (10^{-6} M) in PS/toluene onto a glass substrate were also measured, in a diffraction limited volume, with the same confocal setup used to perform the single molecule experiments, in order to compare these bulk spectra and lifetimes to the single molecule ones. In the latter case, the fluorescence decay profile was built by integrating all photons recorded by the TCSPC card. The integration time was set to 20 s.

2.2. Theoretical section

To calculate spectroscopic properties like the transition dipole moment and the transition energy of the experimentally measured probe molecules (DiIC12 and DiIsty), several quantum chemical approaches have been used. The geometry of the molecule was obtained by using the Hartree–Fock semi empirical Austin Model 1 (AM1) method [21]. Characterization of the lowest electronic singlet excited states has been performed by the semiempirical Hartree–Fock intermediate neglect of differential overlap (INDO) method as parametrized by Zerner et al. [22] This approximation was used in combination with a single configuration interaction (SCI) methodology. For all calculations, the CI active space has been built by promoting one electron from one of the highest sixty occupied to one of the lowest sixty unoccupied levels. Every molecular dynamics simulation has been performed at a constant number of particles, volume and standard temperature (NVT) ensemble. The simulations have been performed at a temperature of 300 K for 500 ps. The configuration of the system has been extracted every 1 ps. The energy was separated in several contributions. The total energy and van der Waals energy have been used in our discussion. These molecular dynamics simulations were performed with the material studio package by Accelrys Software Inc. We have used the universal force field (UFF) [23] in Forcite Studio and a standard cutoff has been kept at 12.5 Å. The radiative lifetime in vacuum has been calculated with the usual formula

$$\tau_0 = \frac{m_e \varepsilon_0 c_0^3}{2e^2 \pi \nu_0 f} \quad (1)$$

by further taking into account the renormalization of the photon in the medium: $\varepsilon_0 \to \varepsilon_r \varepsilon_0$ and $c_0 \to c_0/n$ and the slight change in the transition frequency. In this formula, e is the charge of the electron, ε_0 and c_0 are the permittivity and the speed of light in a vacuum, and ν_0 and f are the transition frequency and the oscillator strength of the probe molecule in a vacuum, respectively. Finally, the polarizabilities were determined by a sum over states (SOS) method encompassing all states involved in the CI space just mentioned.

3. Results and discussion

Fig. 1b shows the normalized absorption and emission spectra of both types of probe molecules in a toluene solution, as measured on the spectrofluorometer. The black curves correspond to the spectra of DiIC12 and the red curves to the spectra of DiIsty. The fluorescence spectrum of DiIsty is significantly broader, is slightly red shifted (10 nm) and has a more intense 0–1 vibronic peak compared to the one of DiIC12. The blue line represents the emission spectrum of DiIC12 in a PS bulk film, i.e. obtained by spin-coating a solution of DiIC12 (10^{-6} M) in PS/toluene (10 mg/ml) onto a glass substrate. It was measured by use of the confocal setup, used in the same conditions as the ones set to perform the single molecule experiments, for the sake of comparison both with the results of these experiments (see hereafter) and with those obtained in solution. The figure clearly exhibits spectra of identical shape but with a slight blue shift (around 5 nm) of the normalized emission spectrum of DiIC12 in a PS bulk film as compared to DiIC12 in a toluene solution. The fluorescence decay profile of the same diffraction limited volume of DiIC12 in the PS bulk film is shown in Fig. 1c (top). It is best fitted (as checked by careful examination of the χ^2 parameter, visual inspection of the residuals and autocorrelation of the latter) by a bi-exponential decay model with decay times $\tau_1 = 1.8$ ns and $\tau_2 = 2.8$ ns with amplitudes of 2.17 and 0.34, respectively. This corresponds to a contribution of 80% of $\tau_1 = 1.8$ ns and 20% of $\tau_2 = 2.8$ ns

Single molecule measurements were performed on thin films, spincoated from a 10^{-9} M solution of DiIsty/DiIC12 in PS/toluene. To localize the single molecules, an area of 10 μm by 10 μm was scanned. Taking into account the number of molecules found in this area and comparing with the expected number to be found for such a low dye concentration (10^{-9} M), we made sure to have the right concentration to measure single molecules. Furthermore, the diffraction limited spots observed on the scanning areas (not shown) confirm the observation of single molecules. Once localized, a fluorescence lifetime trajectory and a fluorescence spectrum were recorded for each individual molecule. Fig. 1c shows the decay profiles, obtained by integrating all photons recorded for two individual DiIC12 molecules (until they get irreversibly photo dissociated) in PS. Both decay curves could be best fitted by a single exponential model with $\tau = 2.8$ ns (middle) and $\tau = 1.8$ ns (bottom). For DiIsty in PS, the fluorescence spectra and lifetime trajectories, obtained by building and fitting with a single exponential model the successive decay profiles in bins of 100 ms, of two different molecules are shown in Fig. 2. One molecule has an average fluorescence lifetime $\tau = 2.6$ ns (Fig. 2a), while the other one has a shorter fluorescence lifetime $\tau = 1.7$ ns (Fig. 2c) as best represented by the mean of the distribution plotted on the right axes in Fig. 2(a,c). In the latter case ($\tau = 1.7$ ns), the corresponding fluorescence spectrum is characterized by an increased amplitude of the 0–1 vibronic peak (Fig. 2d) with respect to the first molecule (Fig. 2b).

For each investigated sample, consisting of either DiIC12 or DiIsty in either non annealed or annealed PS film, more than 150 individual molecules were measured. Every molecule with a low fluorescence lifetime was found to have an emission spectrum with an increased amplitude of the 0–1 vibronic peak, while the intensity of this peak is much lower for a molecule with a longer fluorescence lifetime. This correlation was found for all molecules of DiIsty or DiIC12 embedded in annealed or non annealed PS films and suggested the existence of at least two different species (conformers) for both DiIC12 and DiIsty. Fig. 3 shows a scatter plot of vibronic strength against lifetime together with the distributions of lifetime and vibronic strength for all measured molecules. The vibronic strength is measured here as the maximum intensity of the 0–1 vibronic peak, giving an idea of the coupling with the high frequency modes of the molecule. Clearly, the distribution shows two peaks, one around $\tau = 1.7$ ns with a strong vibronic coupling and one around $\tau = 2.7$ ns with a weak vibronic coupling. Also, the steady state emission spectra in solution (Fig. 1b) showed that the intensity of the 0–1 vibronic peak of DiIsty is larger than the one of DiIC12, already indicating that the common conjugated part of these two types of molecules might adopt a different conforma-

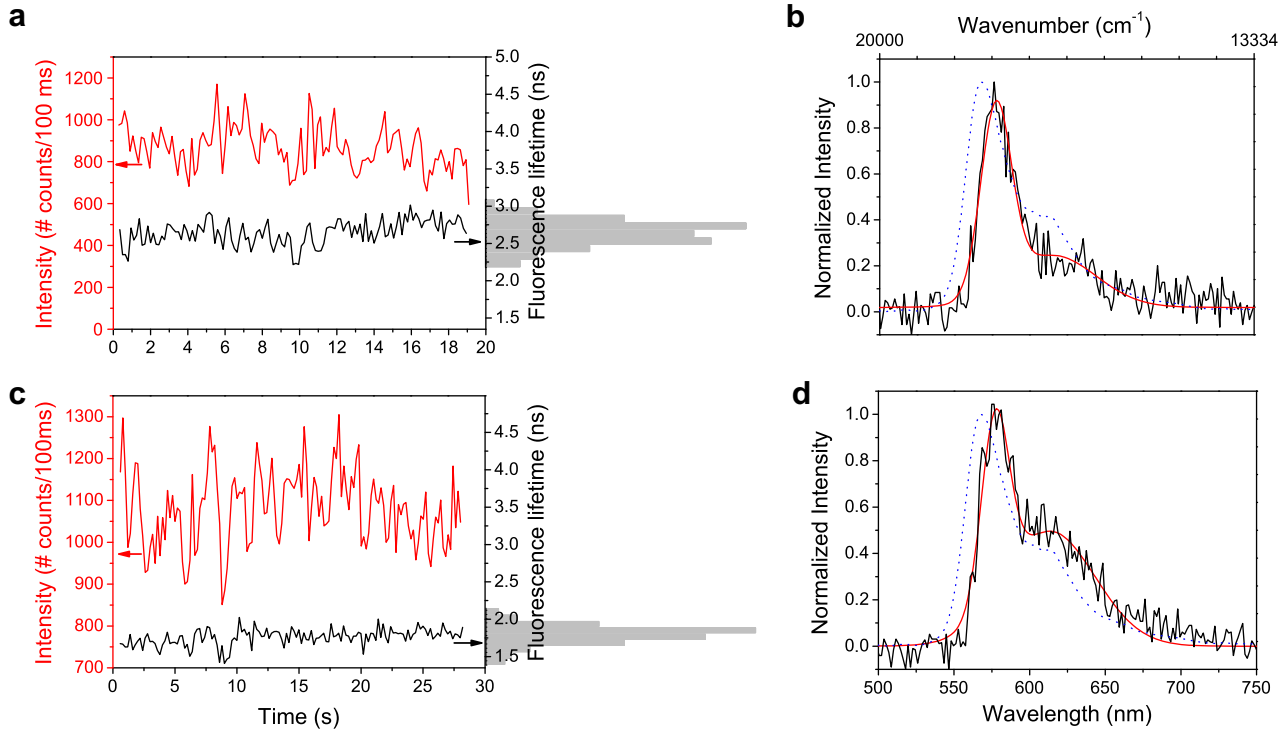

Fig. 2. Intensity and fluorescence lifetime trajectories (a, c) and corresponding fluorescence spectra (b, d) of a molecule with a long fluorescence lifetime (a, b, $\tau \approx 2.8$ ns) and a molecule with a short fluorescence lifetime (c, d, $\tau \approx 1.8$ ns). The blue dotted line in the fluorescence spectra shows the emission spectrum of a diffraction limited volume of the film obtained after spincoating a bulk solution of DiIC12 in PS/toluene on a glass substrate. (For interpretation of the references to color in this figure legend, the reader is referred to the web version of this article.)

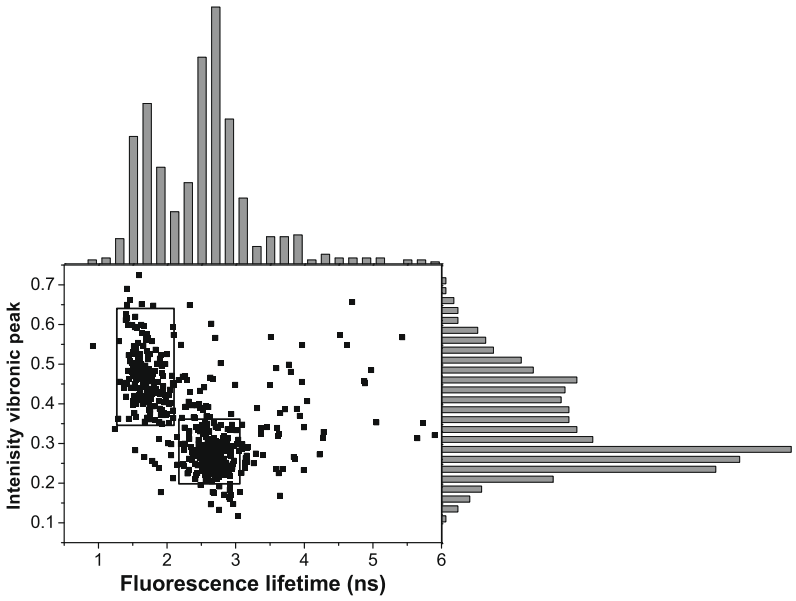

Fig. 3. Scatter plot of the intensity of the 0–1 vibronic peak against the fluorescence lifetime together with their respective distributions for all molecules measured in our investigations. Two clouds can be found, indicated by the surrounding rectangles: one around $\tau = 1.7$ ns with a strong vibronic coupling and one around $\tau = 2.7$ ns with a weak vibronic coupling, thus indicating the clear correlation between these two observables.

tion in solution. Furthermore, a closer look to the emission spectra shown in Fig. 2 (b and d, blue line) and to the decay profile shown in Fig. 1c (top) of DiIC12 in a bulk PS film compared to the emission spectra (Fig. 2b and d) and lifetimes (Fig. 1c middle, bottom) of both types of molecules taken individually clearly indicated that the measured diffraction limited volume of DiIC12 in a bulk PS film is constituted of the two populations just mentioned.

The distributions of the mean fluorescence lifetimes obtained from each individual trajectory are shown in Fig. 4. They all have a bimodal character with peaks centered around $\tau \approx 1.7$ ns and $\tau \approx 2.6$ ns. For DiIC12 non annealed (Fig. 4a) most molecules (80%) show an average lifetime of 2.6 ns, while only a minor fraction (20%) of the molecules exhibits a shorter mean lifetime of about 1.7 ns. For DiIsty in a non annealed sample (Fig. 4b), we

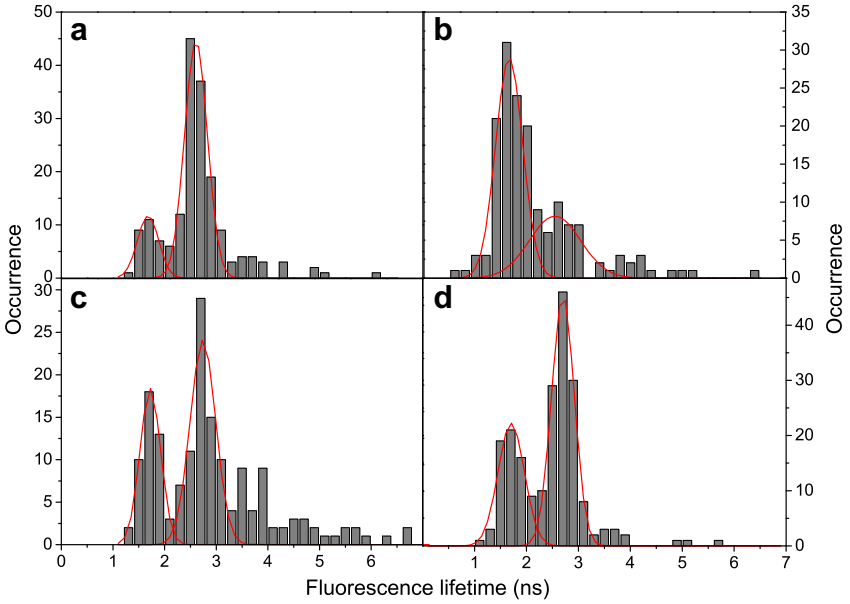

Fig. 4. Bimodal distribution of fluorescence lifetimes for DiIC12 not annealed (a) and annealed (c) and DiIsty not annealed (b) and annealed (d). All distributions are fitted with a double Gaussian which gives for (a): 20% (80%) of the molecules with an average fluorescence lifetime of 1.7 ns (2.6 ns), for (b): 65% (35%) of the molecules with an average fluorescence lifetime of 1.5 ns (2.5 ns), for (c): 38% (62%) of the molecules with an average fluorescence lifetime of 1.7 ns (2.7 ns), for (d) 36% (64%) of the molecules with an average fluorescence lifetime of 1.7 ns (2.7 ns). Only the molecules which show a clear correlation between their fluorescence lifetime and spectrum are taken into account in the Gaussian fits (molecules with a fluorescence lifetime $\tau > 3.5$ ns are not considered).

observe an opposite situation with only 35% of the molecules having a longer fluorescence lifetime. After annealing, allowing for a general relaxation of the matrix and release of the eventual stresses remaining from the spin-coating process, the same type of bimodal distribution is obtained, with a low proportion of molecules having a shorter fluorescence lifetime both for DiIC12 (38%, Fig. 4c) and DiIsty (36%, Fig. 4d).

In order to tentatively assign the origin of each couple of fluorescence lifetime, spectrum to a particular conformer of the common conjugated core, we performed theoretical calculations. DiI possesses four double bonds between the nitrogen atoms (Fig. 1a) of which the configuration can be *cis* (C) or *trans* (T). Due to steric constraint, only 3 of the $2^4 = 16$ possible conformers have been analyzed in our study, the ones that have the highest Boltzmann's occurrence to be observed. The three selected conformers (CTTC, TTTC and TTTT) can be described by the two dihedral angles ϕ_1 and ϕ_2 (see Fig. 5a). The conformers can be expressed by couples as $[\phi_1;\phi_2]$ which gives $[18^\circ;0^\circ]$ for CTTC (steric hinder does not allow a pure planar conjugated DiI core and the minimum angle obtained at AM1 level for all studied molecules is circa 18°), $[180^\circ;0^\circ]$ for TTTC and $[180^\circ;180^\circ]$ for TTTT (Fig. 5a). Instead of using the real systems DiIC12 and DiIsty, model compounds DiIC6 (hexyl alkyl chains instead of dodecyl chains) and DiIPh3 (oligomers of three styrene units instead of 23 units) have been used to keep a reasonable number of degrees of freedom.

Radiative lifetimes computed using the INDO/SCI semi empirical method for variable (18° steps) ϕ_1 and ϕ_2 angles are plotted in Fig. 5b. For both types of substituents (C6 or Ph3) the CTTC conformer exhibits the longest computed radiative lifetime. TTTC has an intermediate value and TTTT is characterized by the shortest radiative lifetime. This can be explained by the strength of the transition dipole moment which is highest for TTTT and weakest for CTTC. For each conformer, the geometry optimization has been performed at the AM1 level of theory. Each exact value of the four torsion angles between the nitrogen atoms has been frozen in order to calculate each energy minimum. On each partially frozen geometry, a molecular dynamics simulation is performed for 500 ps at 300 K in the NVT ensemble. After each ps of the runs, the van der Waals contribution to the total energy is extracted and stored. For both types of substituents the CTTC conformer is the most stable and its van der Waals contribution is the smallest (3 kcal/mol for DiIC6 and around 8 kcal/mol for DiIPh3), as shown in Table 1. Let us note here that, in a molecular modeling approach, the computed van der Waals energy is the sum of all repulsive (sterical hindrance at short distance, important in our case) and attractive components, at longer distance (the classic vdW chemical point of view).

For CTTC, the alkyl and phenyl substituents (the arms) are on the same side of the conjugated core, which means that intramolecular interactions between the arms can occur. The TTTT conformer also has the arms on the same side, but the distance in between them is too large to have a strong intramolecular interaction. For TTTC the arms are on different sides which avoids any interaction. The steric hinder in the conjugated core of CTTC can be seen as a catalyst for the strong intramolecular interaction which will stabilize the overall system.

By comparing the theoretical calculations to the experimental results, it is clear that for DiIsty in a non annealed film, the TTTC or TTTT conformer must be the most abundant since most molecules have a shorter lifetime. In contrast, for the three other samples (both annealed films and DiIC12 in a non annealed film) the most abundant conformer must be CTTC, which is the one with the longest fluorescence lifetime.

For the non annealed samples, the memory of the dye molecule conformation in the solvent is retained since the short (long) lifetime $\tau \approx 1.7$ ns ($\tau \approx 2.6$ ns) exhibited by most molecules of DiIsty (DiIC12) in the non annealed film (Fig. 4b, respectively Fig. 4a) correlates with the enhanced (reduced) 0–1 vibrational peak of their fluorescence spectra and match the results obtained for DiIsty (DiIC12) in a toluene solution (Fig. 1b). A decay profile of both types of dyes in solution will not be enlighting since the internal conversion processes allowed in such a mobile surrounding lead to a drastic reduction of the observed lifetime. For the conformers TTTC and TTTT the interaction between the arms is weak, which favors their respective interaction with the solvent. The interaction between the oligostyrene chains and toluene is stronger than be-

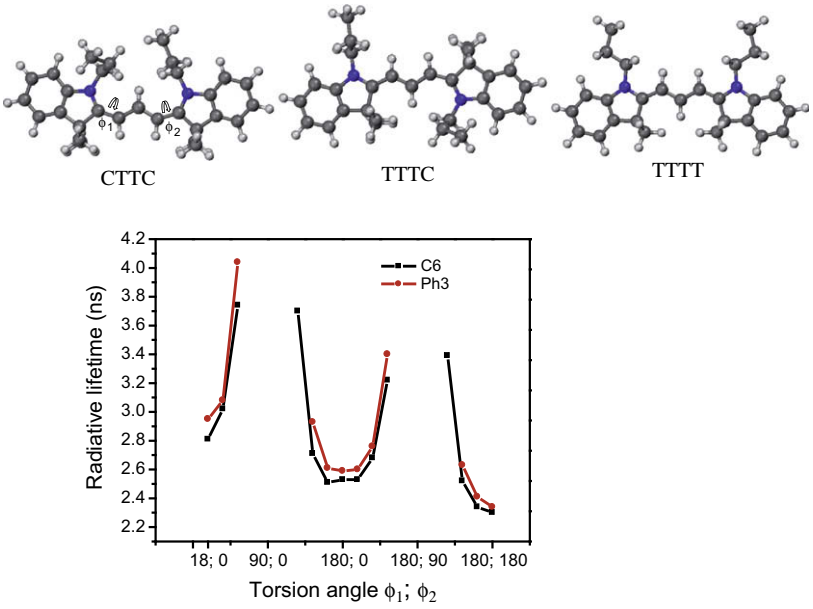

Fig. 5. (a) Schematics of three conformers of DiI having the highest Boltzmann's occurrence to be observed. The dihedral angles ϕ_1 and ϕ_2 taken into account in the discussion are depicted on the CTTC conformer. (b) Radiative lifetimes as a function of peculiar values of the pairs of angles $(\phi_1;\phi_2)$ for both types of molecules (C6 in black for DiIC12, and Ph3 in red for DiIsty). For both types, CTTC shows the longest radiative lifetime, TTTT the shortest one and TTTC has an intermediate value. (For interpretation of the references to color in this figure legend, the reader is referred to the web version of this article.)

Table 1
Calculated radiative lifetime and average van der Waals energy of the different conformers.

		Radiative lifetime (ns) AM1 geometries	Dye substituent contribution Average value (minimum; maximum) (kcal/mol) Molecular dynamic
C6			
	CTTC	2.8	26.6 (23.7; 28.8)
	TTTC	2.5	29.2 (24.1; 31.2)
	TTTT	2.3	30.0 (24.2; 31.8)
Ph3			
	CTTC	3.0	64.6 (58.1; 71.4)
	TTTC	2.6	74.0 (67.0; 81.0)
	TTTT	2.4	72.5 (64.2; 82.0)

tween the alkyl chains and toluene. Hence, for DiIsty molecules in a non annealed film, the TTTC and TTTT conformations will be favored, which explains the higher fraction of molecules having a short fluorescence lifetime $\tau \approx 1.7$ ns. The weaker interaction between the alkyl chains and toluene explains the opposite distribution for DiIC12. This corresponds to the steady state spectrum observed for DiIsty (DiIC12) in solution, where it mainly adopts the TTTC and TTTT (CTTC) conformations. After the samples have been annealed, the polymers have had time to relax and reorganize, the solvent memory is lost and the dye molecules will adopt the most stable CTTC conformation.

4. Conclusions

DiIC12 and DiIsty can adopt different conformations in a poly(styrene) matrix, in non annealed as well as in annealed samples. Experimentally, the evidence for the existence of at least two different conformers was found both in the bi-exponential model necessary to fit the decay profile at the bulk level and in the bimodal character of the fluorescence lifetime distributions found at the single molecule level. These distributions are different for both dyes in the non annealed samples and get similar after annealing. Owing to quantum chemical calculations, different conformations could be assigned to the observed values (mainly two) of the fluorescence lifetime. The two dyes, having a common conjugated core, but with different side chains grafted on the nitrogen atoms, adopt different conformations in the non annealed samples, due to the specific interactions of these side chains with the surrounding medium (competition between intra- and inter- molecular interactions). The strong interactions between oligostyrene and toluene favors the TTTT and TTTC conformers of DiIsty in solution and in the non annealed sample. The interactions between the alkyl chains and toluene are weaker, so that the CTTC conformer of DiIC12 is observed in solution and in the non annealed sample. After annealing, allowing for a complete relaxation of the polymer medium surrounding the dyes, CTTC, the most stable conformer, appears as the most abundant, and the same fluorescence lifetime distributions are obtained for both dye molecules. It is clear that the side chains can play a role in the interaction with the polymer. However, the nature of the side chains only matters for the non annealed samples, i.e. in a non equilibrium system. After annealing, when the matrix has relaxed, i.e. after having reached an equilibrium, the most stable conformer is mostly observed. As the type of conformer found in the matrix and its interaction with the surrounding chains governs the local packing of the matrix and thus its local free volume, the results and perspectives of such investigations might give some new insight to the plasticizing effect as a function of temperature change and ageing.

Acknowledgements

The authors are thankful to the FWO for financial support and a postdoctoral fellowship to R.V., to the research council of K.U. Leuven for funding in the framework of GOA 2006/2, and to Belgian Science policy for funding through IAP V/03 and VI/27/. The 'Instituut voor de aanmoediging van innovatie door Wetenschap en Technologie in Vlaanderen' (IWT) is acknowledged for Grant ZWAP 04/007 and for a fellowship to E.B. D.B. is a research director of the FNRS.

References

[1] X.S. Xie, J.K. Trautman, Annu. Rev. Phys. Chem. 49 (1998) 441.
[2] F. Cichos, C. von Borczyskowski, M. Orrit, Curr. Opin. Colloid Interface Sci. 12 (2007) 272.
[3] J.N. Clifford et al., J. Phys. Chem. B 111 (2007) 6987.
[4] A. Schob, F. Cichos, J. Schuster, C. von Borzyskowski, Eur. Pol. J. 40 (2004) 1019.
[5] L.A. Deschenes, D.A. Vanden Bout, J. Phys. Chem. B 106 (2002) 11438.
[6] R. Zondervan, F. Kulzer, G.C.G. Berkhout, M. Orrit, Proc. Natl. Acad. Sci. USA 104 (2007) 12628.
[7] R. Zondervan, T. Xia, H. van der Meer, C. Storm, F. Kulzer, W. van Saarloos, M. Orrit, Proc. Natl. Acad. Sci. USA 105 (2008) 4993.
[8] B. Sick, B. Hecht, L. Novotny, Phys. Rev. Lett. 85 (2000) 4482.
[9] A.P. Bartko, K. Xu, R.M. Dickson, Phys. Rev. Lett. 89 (2002) 026101.
[10] H. Uji-i et al., Polymer 47 (2006) 2511.
[11] M. Böhmer, J. Enderlein, J. Opt. Soc. Am. B 20 (2003) 554.
[12] M.A. Lieb, J.M. Zavislan, L.J. Novotny, J. Opt. Soc. Am. B 21 (2004) 1210.
[13] R.M. Dickson, D.J. Norris, W.E. Moerner, Phys. Rev. Lett. 81 (1998) 5322.
[14] R.A.L. Vallée, M. Van der Auweraer, F.C. De Schryver, D. Beljonne, M. Orrit, ChemPhysChem 6 (2005) 81.
[15] R.A.L. Vallée, M. Baruah, J. Hofkens, F.C. De Schryver, N. Boens, M. Van der Auweraer, D. Beljonne, J. Chem. Phys 126 (2007) 184902.
[16] R.A.L. Vallée, N. Tomczak, L. Kuipers, G.J. Vancso, N.F. van Hulst, Phys. Rev. Lett. 91 (2003) 038301.
[17] N. Tomczak, R.A.L. Vallée, E.M.H.P. van Dijk, M. García-Parajó, N. van Hulst, G.J. Vancso, Eur. Pol. J. 40 (2004) 1001.
[18] R.A.L. Vallée et al., J. Am. Chem. Soc. 127 (2005) 12011.
[19] R.A.L. Vallée, M. Van der Auweraer, W. Paul, K. Binder, Phys. Rev. Lett. 97 (2006) 217801.
[20] M. Maus, J. Hofkens, T. Gensch, F.C. De Schryver, J. Schaffer, C. Seidel, Anal. Chem. 73 (2001) 2078.
[21] M.J.S. Dewar, E.G. Zoebisch, E.F. Healy, J.J.P. Stewart, J. Am. Chem. Soc. 107 (1985) 3902.
[22] M.C. Zerner, G. Loew, R. Kichner, U.T. Mueller-Westerhoff, J. Am. Chem. Soc. 122 (2000) 3015.
[23] A.K. Rappe, C.J. Casewit, K.S. Colwell, W.A. Goddard III, W.M. Skiff, J. Am. Chem. Soc. 114 (1992) 10024.